ANISOTROPIC ELECTRIC PROPERTIES OF PURPLE MEMBRANE AND THEIR CHANGE DURING THE PHOTOREACTION CYCLE

YOSHIAKI KIMURA, MASAKO FUJIWARA, AND AKIRA IKEGAMI
The Institute of Physical and Chemical Research, 2-1 Hirosawa, Wako-shi, Saitama 351, Japan

ABSTRACT Purple membrane suspension shows two different orientations in electric fields of different frequencies. The orientation at low frequencies ($\leq\sim$10 Hz), with the membrane surface perpendicular to the electric field, is due to permanent dipole moment of the membrane and the orientation at high frequencies ($\geq\sim$100 Hz), with the surface parallel to the electric field, is due to induced dipole moment. By quantitative analysis of these orientations, we determined the permanent dipole moment and the polarizability. Both values varied according to the membrane size: the permanent dipole moment ranged from 500 kD to 10 MD and was proportional to the square of the diameter of the membrane. The polarizability ranged from 1×10^{-13} to 1×10^{-11} cm^3 and was proportional to the third to fourth power of the diameter. Because the permanent dipole moment was proportional to the area of the membrane, we could determine permanent dipole moment per bacteriorhodopsin. By determining the actual membrane size under electron microscopy, we got 98 D/bacteriorhodopsin. We also concluded that the direction of the permanent dipole moment was from the cytoplasmic to the extracellular side. These values, however, were strongly dependent on the ionic strength in the medium, suggesting a screening effect due to counter ions near the membrane surface. We evaluated the screening effect and showed about a four-charge difference between the two sides of the purple membrane. Under illumination, we found that the permanent dipole moment decreased from 98 to 63 D/bacteriorhodopsin. From the best-oriented sample, we also concluded that the angle of retinal against the axis normal to the membrane surface was >68.6°.

INTRODUCTION

Purple membranes are specialized regions in the plasma membrane of *Halobacterium halobium* that function as light-energy converters (1, 2). Purple membrane is composed of lipids and a single species of protein, bacteriorhodopsin. The bacteriorhodopsin contains a chromophore, one molecule of retinal, bound to a lysine residue and has a strong absorption band around 570 nm. Trimeric clusters of bacteriorhodopsin molecules form a hexagonal lattice in the purple membrane. For reviews see references 3–5.

Purified purple membranes can be suspended in the form of sheets. The suspension becomes dichroic in electric fields (6–11). This electric dichroism reflects the electrically anisotropic properties of the membrane. The anisotropic properties are important because they determine its function, the light-driven translocation of protons across the membrane. An analysis of the electric dichroism may, therefore, help us to understand the transport process. We have reported briefly (11) that the membranes orient perpendicular to the electric field at frequencies $<\sim$10 Hz and parallel to it $>\sim$100 Hz, and attributed the low-frequency orientation to the permanent dipole moments and the high-frequency orientation to the polarizability or to the resultant induced dipole moments. Similar results had already been obtained by Saigo (7) and Keszthelyi (8), who also gave values for the permanent dipole moment. But they ignored the polarizability and the size distribution of the membrane sheets. In addition, technical problems, due to electrode polarization and effects of light scattering, were not taken into account.

Here we first analyze rigorously the frequency dependence of the electric dichroism and justify the interpretation on which the further quantitative analyses are based. The results support the interpretations that we gave before (11). Then we determine the values of the permanent dipole moment and the polarizability. We show the dependence of these values on membrane size and calculate the permanent dipole moment per bacteriorhodopsin molecule. The effects of ion concentration and a screening effect due to counter ions are evaluated. We also demonstrate a relatively large change of the permanent dipole moment of bacteriorhodopsin during the photoreaction cycle.

MATERIALS AND METHODS

Purple membrane was purified from *Halobacterium halobium* R_1M_1. The culture conditions and purification procedures were essentially the same as those of Oesterhelt and Stoeckenius (12). Purified purple membranes were checked by sodium dodecyl sulfate (SDS) polyacrylamide gel electrophoresis and showed a single peak.

These purple membranes, however, have a variety of sizes. To get membrane fractions of homogeneous size, we used the following procedures. First, the membranes were fractionated by rate centrifugation in a sucrose density gradient. Each fraction was washed with distilled water three times. Next, the membranes were passed through a Nuclepore

membrane (Pleasanton, CA, diameter of pores: 1.0, 0.8, 0.6, 0.4, 0.2, and 0.1 μm). To produce small purple membranes, we sonicated samples before the fractionation by using a tip sonicator (Chouonpa Industry Co. Ltd., Tachikawa, Japan; 10 kHz, 150 W) for 20 or 60 min at less than maximum power. The first sucrose density gradient step was sometimes skipped without a significant difference. Purple membranes were fractionated immediately after purification and were used within 1 mo.

For the electric dichroism, suspensions were prepared as follows. Purple membranes were refiltered through the Nuclepore membrane just before use to remove possible aggregates. The concentration was adjusted to <6 μM protein. Then, salt or buffer was added; the final concentration was 1 mM NaCl for the experiments of the membrane-size dependence and the effect of trypsin treatment, 0.1 mM phosphate buffer (pH 7.0) for the salt effect experiment, 1 mM phosphate buffer (pH 7.0) without adding other salt for the illumination experiments. Finally, these suspensions were bubbled with nitrogen for 5 min and was used in the nitrogen stream. Temperature was set at 4°C except for some cases indicated in the figure legends. Trypsin treatment was done according to Gerber et al. (13) and the amount of peptide removed from the membrane was checked with fluorescamine (Roche, Basel, Switzerland).

The apparatus and procedures for the electric dichroism measurement were the same as reported before (11). Briefly, platinized platinum electrodes were set parallel to the measuring light path in a cuvette (10 × 10 × 45 mm, inside dimensions). Changes of linear dichroism were measured along this light path and were recorded in a transient recorder (DM305; Iwatsu, Tokyo, Japan). Light-scattering problems were minimized by putting the cuvette close to the window of a end-on type photomultiplier (R374; Hamamatsu Photonix, Hamamatsu, Japan), narrowing the light beam (1 × 7 mm in the center of the cuvette), and confining the concentration to <6 μM. This concentration also helped to minimize membrane-membrane interactions. The electrodes were freshly platinized no longer than 24 h before the experiments. The applied electric fields were reversing rectangular pulses between 0.07 Hz and 28 kHz (0–110 V/cm) or sinusoidal fields between 0.01 Hz and 3 MHz (0–15 V/cm). The actual electric field was measured with a pair of capillary electrodes. The deviations of the actual electric field from the applied electric field were <5%.

For illumination experiments, we used a thin cuvette (inside dimension 2 × 10 × 45 mm) set at an angle of 45° to the measuring beam (Fig. 15 *a*). As for the illuminating light, we used a 700-W tungsten projector. The light was filtered by 2% $CuSO_4$ solution and a yellow filter (O52; Hoya Glass Works Ltd., Tokyo, Japan). The stray light and light scattering from the illumination were estimated by measuring signals with the measuring light off and were subtracted from the original signals.

Actual sizes of purple membranes were determined by electron microscopy. We calculated the average diameter of purple membranes as follows. First, we regarded a membrane on the electronmicrograph as an ellipse with axes of $2a$ and $2b$ and counted the population of $(4ab)^{1/2}$, where the $(4ab)^{1/2}$ corresponds to a diameter of a circle of the same area with the ellipse. Next, we calculated the average diameter according to the following equation:

$$\bar{x} = \frac{\int x\omega(x)f(x)\mathrm{d}x}{\int \omega(x)f(x)\mathrm{d}x} \approx \frac{\sum x_i\omega(x_i)f(x_i)}{\sum \omega(x_i)f(x_i)}, \quad (1)$$

where x is $(4ab)^{1/2}$, $\omega(x)$ is the weight function (x^6), and $f(x)$ is the distribution function of x. The weight function $\omega(x)$ was determined as follows. Because the absorption is proportional to the area of the membrane, we needed x^2. Furthermore, in the measurement of electric dichroism, only oriented purple membranes contribute to the dichroism. The dichroism is proportional to the square of the permanent dipole moment or to the polarizability in weak electric fields, and the permanent dipole moment is proportional to the square of the diameter of the membrane and the polarizability is proportional to the 3rd–4th power of the diameter, which were confirmed in Results. So another x^4 was needed to the weight function. Thus we used x^6 for the weight function.

The relaxation time of electric dichroism is related to the membrane size and was used as a measure of the size for each measurement of electric dichroism. There is a theoretical relation between the rotational relaxation time and the radius of a disklike molecule (14). According to Perrin (14), the rotational diffusion constant of a disk is expressed as follows:

$$D = \frac{3kT}{32}\underline{\eta} \cdot \frac{1}{c^3}, \quad (2)$$

where c is the radius of the disk, $\underline{\eta}$ is the viscosity of the medium, k is the Boltzmann constant and T is the temperature. The rotational diffusion constant D is related to the relaxation time τ by

$$\tau = \frac{1}{6D}. \quad (3)$$

This means that τ is proportional to the third power of c. First, we confirmed the theoretical relation between the diameter determined by electron microscopy and the relaxation time. Then we calculated membrane sizes from relaxation times by using the relation.

When we calculated the permanent dipole moment per bacteriorhodopsin, we determined the number of bacteriorhodopsin per one membrane sheet by dividing the area of the membrane by the area per bacteriorhodopsin, 1,145.8 A^2 (15).

THEORY

To evaluate electric dichroism, we calculated the electric anisotropy, $S_\parallel - S_\perp$. Definitions of $S_\parallel$ and $S_\perp$ are as follows:

$$S_\parallel = \frac{A_\parallel(E) - A}{A}; \qquad S_\perp = \frac{A_\perp(E) - A}{A}, \quad (4)$$

where A is the absorption in the absence of electric field and $A_\parallel(E)$ and $A_\perp(E)$ are absorptions in the presence of electric field, E. The subscripts $_\parallel$ and $_\perp$ mean that the absorption was measured by using polarized light, parallel and perpendicular to the direction of the electric field. When E equals zero, $S_\parallel = S_\perp = 0$ is satisfied because of $A_\parallel(0) = A_\perp(0) = A$. Furthermore, given that rotational symmetry around the direction of the electric field is assured and the extinction coefficient does not change, the following equations are easily derived:

$$S_\parallel + 2S_\perp = 0; \quad (5)$$

$$S_\parallel - S_\perp = \frac{3}{2} \cdot S_\parallel. \quad (6)$$

Eq. 5 was used to establish that the extinction coefficient did not change under our experimental conditions.

When a particle has axial symmetry, the orientation of the particle can be described relative to orientation of the axis. In such a case, the electric anisotropy, $S_\parallel - S_\perp$, is described by

$$S_\parallel - S_\perp = \Theta \cdot \Psi, \quad (7)$$

where Θ is the angle factor of the sample and is related to the angle, γ, between the absorption transition moment of the chromophore and the axis of symmetry, and Ψ is the orientation factor of the sample and is related to the angle, θ, between the axis of symmetry and the direction of the electric field. The relations are

$$\Theta = 3 \cdot P_2(\cos\gamma); \ \Psi = \langle P_2(\cos\theta)\rangle, \quad (8)$$

where $P_2(x)$ denotes the second Legendre function $[P_2(x) = (3x^2 - 1)/2]$ and $\langle\ \rangle$ denotes an average for all membranes. If γ remains constant, $S_\parallel -$

$S_\perp$ is proportional to Ψ. This means that the electric anisotropy reflects a rotational motion of the membrane in the electric field.

To describe Ψ more explicitly, we need to know the angular distribution of the axis of symmetry. Here we define $f(\theta, t)$ as an angular distribution function of the axis at a given time t. This $f(\theta, t)$ follows the rotational diffusion equation in the presence of a torque M:

$$\frac{\partial f}{\partial t} = D\nabla^2 f - \mathrm{div}\left(f \cdot \frac{M}{\xi}\right), \tag{9}$$

where D is the rotational diffusion coefficient, ∇^2 is the Laplace operator for angle, M is the torque that the membrane receives in the electric field and ξ is the rotational friction coefficient. The torque M can be calculated from the potential energy that the membrane has in the electric field as

$$M = \frac{\partial U}{\partial \theta}, \tag{10}$$

where U is the potential energy, which can be expressed as follows, assuming the membrane has a permanent dipole moment along the axis of symmetry and has a polarizability whose principal axis is perpendicular to the axis of symmetry:

$$U = -\mu E\cos\theta - \frac{1}{2} \cdot (\alpha_1 - \alpha_2)E^2\cos^2\theta, \tag{11}$$

where μ is the excess permanent dipole moment and α is the excess polarizability which causes induced dipole moment. Subscript 1 denotes the direction of the axis of symmetry and 2 denotes the submajor axis perpendicular to 1. Then, $\Psi(t)$ can be described by using this $f(\theta, t)$ as follows:

$$\Psi = 2\pi \int_0^\pi P_2(\cos\theta) f(\theta, t)\sin\theta \mathrm{d}\theta. \tag{12}$$

Benoit solved Eq. 9 for a weak electric field (16). The result was either

$$\Psi(p, q, t) = \Psi(p, q, \infty)\left|1 - \frac{3\kappa}{2(\kappa + 1)}\exp(-2Dt) + \frac{\kappa - 2}{2(\kappa + 1)}\exp(-6Dt)\right| \tag{3}$$

where $\kappa = p^2/q$, $p = \mu E/kT$, and $q = (\alpha_2 - \alpha_1)E^2/kT$, or

$$\Psi(p, q, t) = \Psi(p, q, 0) \cdot \exp(-6Dt), \tag{14}$$

when $E = 0$, which corresponds to the relaxation curve after the electric field is switched off.

Here we describe some characteristics of the orientations due either to pure permanent dipole moment or to pure induced dipole moment, which we can derive from Eqs. 13 and 14. We will use these characteristics for characterizing the orientations of purple membranes. First, the initial slope of the rising curve is

$$\left.\frac{\mathrm{d}\Psi(p, q, t)}{\mathrm{d}t}\right|_{t=o} = \frac{6D}{\kappa + 1} \cdot \Psi(p, q, \infty). \tag{15}$$

Therefore, when the polarizability is negligible compared with the permanent dipole moment ($\kappa \sim \infty$), the initial slope is zero. When the permanent dipole moment is zero ($\kappa = 0$), Eq. 13 gives:

$$\Psi(0, q, t) = \Psi(0, q, \infty)\left|1 - \exp(-6Dt)\right|. \tag{16}$$

This equation is just antisymmetrical to Eq. 14. Second, the area ratio of the rising curve and the relaxation curve (see Fig. 4 inset) is easily calculated from Eqs. 13 and 14 as

$$\frac{S_I}{S_{II}} = \frac{4\kappa + 1}{\kappa + 1}. \tag{17}$$

From this equation, it is concluded that the area ratio reaches 4 as κ approaches infinity, and reaches 1 as κ approaches zero. That is, the area ratio becomes 4 for pure permanent dipole moment orientation and 1 for pure induced dipole moment orientation.

For the analysis of the first change of the frequency dependence (10–100 Hz), we used a sinusoidal electric field. Ogawa and Oka solved Eq. 9 for this case by substituting $E = E_0\cos\omega t$ and assuming small E_0 (17). The results showed that the electric dichroism has double frequency and has some delay in phase. The phase delay, δ, and the amplitude, $2b$, can be easily calculated according to their results:

$$\cos\delta = \frac{1 - 6\tau^2\omega^2}{(1 + 9\tau^2\omega^2)^{1/2} \cdot (1 + 4\tau^2\omega^2)^{1/2}}, \tag{18}$$

$$2b = 3P_2(\cos\gamma) \cdot \frac{3}{5}\left|\frac{\mu E_0}{kT}\right|^2 \cdot \frac{1}{(1 + 9\tau^2\omega^2)^{1/2} \cdot (1 + 4\tau^2\omega^2)^{1/2}}, \tag{19}$$

where $\tau = 1/6D$.

Permanent dipole moment and polarizability was calculated from the voltage dependence of electric dichroism in the weak electric field as follows. The electric anisotropy is related to the angle factor Θ and the orientation factor Ψ as in Eq. 7. Assuming Θ is constant, which is justified in Results, Ψ was calculated by using this relation. There we need $\Theta = -0.9736$ ($\gamma = 70°$).

In equlibrium, $\partial f/\partial t = 0$ in Eq. 9. From Eqs. 9–12, ψ was resolved and was expressed by the permanent dipole moment and the polarizability by Shah (18) in the case of disklike particles, where the permanent dipole moment is perpendicular to the disk surface and the polarizability is dominant along the disk surface. The relation can be approximated as follows:

$$\psi = \frac{1}{15} \cdot E^2 \cdot \left|\frac{|\mu|^2}{|kT|} - \frac{\alpha_2 - \alpha_1}{kT}\right|. \tag{20}$$

This equation applies only when the electric field is weak. We used Eq. 20 after confirming that the electric anisotropy was proportional to the square of the electric field. First, we calculated the polarizability from data at the high frequency by substituting $\mu = 0$ in Eq. 20, and then calculated the permanent dipole moment from data at the low frequency by using the polarizability obtained above.

The expression $S_\parallel - S_\perp$ needs to be modified when the measurement is done in the optical setup as in Fig. 15 *a*. If we define S_h and S_v in a similar way as $S_\parallel$ and $S_\perp$, as in Eq. 4, where the absorptions are measured with horizontally and vertically polarized light, S_h and S_v are related to $S_\parallel$ and $S_\perp$ as follows:

$$S_h = P_2(\cos\phi) \cdot S_\parallel, \tag{21}$$

$$S_v = S_\perp, \tag{22}$$

where ϕ is the angle defined as in Fig. 15 *a*. Because the membranes are suspended in water, ϕ can be easily obtained from Snell's law of refraction: 32.12°. The other analyses are the same as above.

RESULTS

The First Dispersion

Two completely opposite changes of electric dichroism were observed when reversing rectangular electric fields of

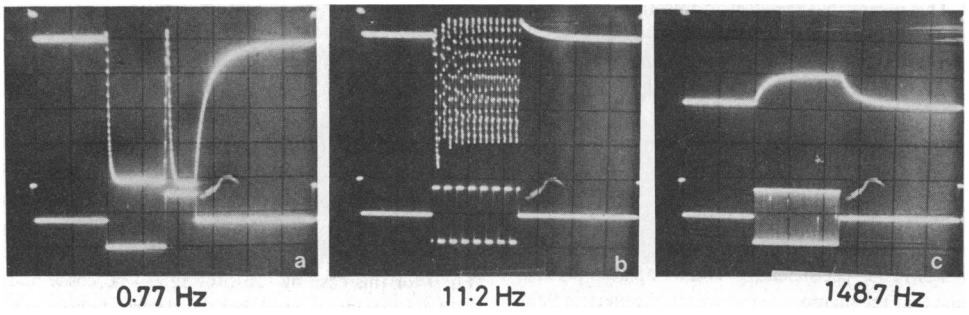

FIGURE 1 Typical curves of electric dichroism of a purple membrane suspension at various frequencies. In each panel, the *upper curve* shows dichroism change ($\Delta I_{\parallel}$ which is almost proportional to $\Delta A_{\parallel}$) and the *lower curve* shows the applied electric field (E). These were measured at 40 V/cm, 20°C in the presence of 1 mM NaCl under a nitrogen stream.

various frequencies were applied to purple membrane suspensions (Figs. 1 and 2). Upper and lower envelopes of oscillations and plateaus plotted against frequency clearly show the frequency region where the first electric anisotropy dispersed (Fig. 2). This dispersion is explained quantitatively later in this section.

Characteristics of the Time-Courses of Electric Dichroism

First, $S_{\parallel}$ was exactly twice as large as $S_{\perp}$ in magnitude and the two had opposite signs to each other (data not shown). From this relation we concluded that there was no change in the absorption extiction coefficient. Second, the initial slopes of rising curve were almost zero at the low frequency (Fig. 3*a*) and were not at the high frequency (Fig. 3*b*). Furthermore, the rising curve at the high frequency were antisymmetrical to the relaxation curve (Fig. 1). Third, the initial ratios of the rising curve area and the relaxation curve area were 4 at the low frequency and 1 at the high frequency (Fig. 4). Both ratios decreased as the electric field intensity increased. Fourth, there appeared sharp dips at the reversing point of the electric field at the low frequency but no change occurred at the high frequency (Fig. 1). In summary, all features at the low frequency indicate the orientation due to pure permanent dipole moment and all features at the high frequency indicate the orientation due to pure induced dipole moment (see Theory).

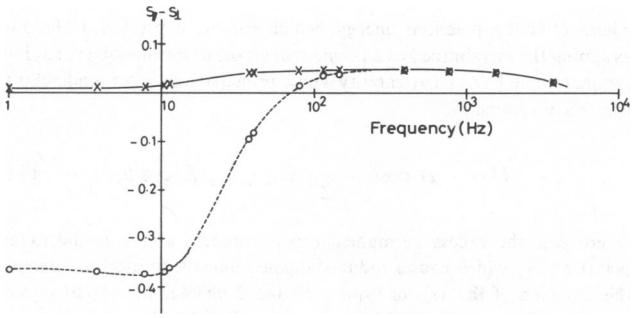

FIGURE 2 The upper contour (x) and lower contour (O) of the dichroism change in Fig. 1 plotted against the frequencies. $\Delta I_{\parallel}$ was transformed to the electric anisotropy, $S_{\parallel} - S_{\perp}$.

Analysis by Use of Sinusoidal Electric Fields of Various Frequencies.

When an electric field $E = E_0 \cos\omega t$ was applied to a purple membrane suspension, the observed dichroism also showed a sinusoidal change but with double frequency and phase delay (Fig. 5*a*, *b*). To show the phase delay more clearly,

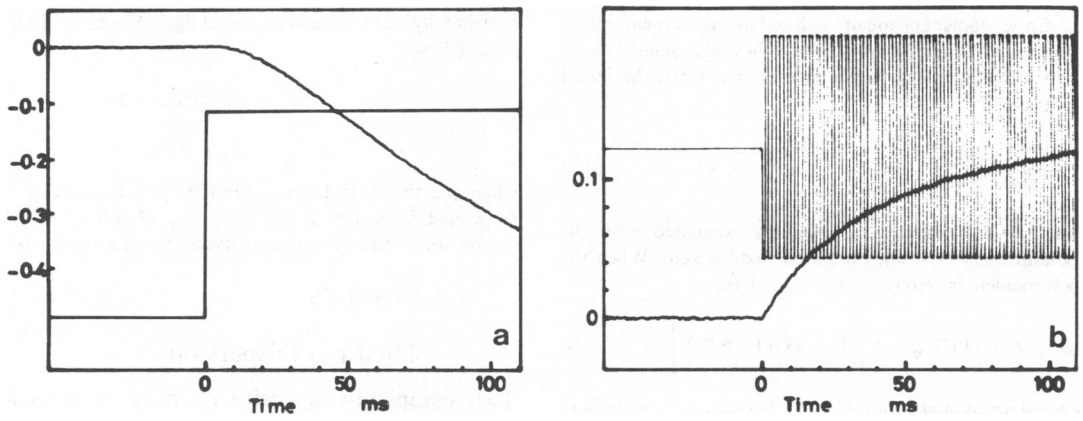

FIGURE 3 Initial rising slope of dichroism change. (*a*) 0.77 Hz. (*b*) 393.3 Hz.

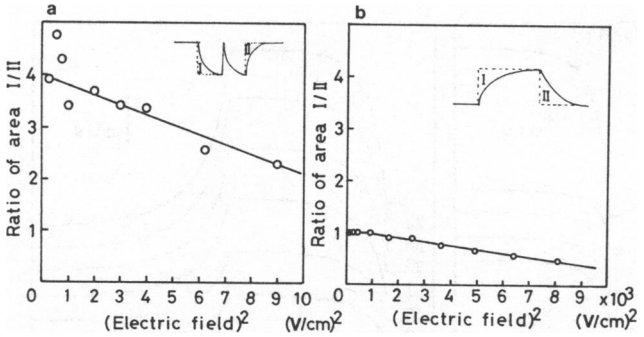

FIGURE 4 Ratio of areas (I/II) drawn by the rising curve (I) and the relaxation curve (II). *Insets* show areas I and II. (*a*) 0.77 Hz. (*b*) 393.3 Hz.

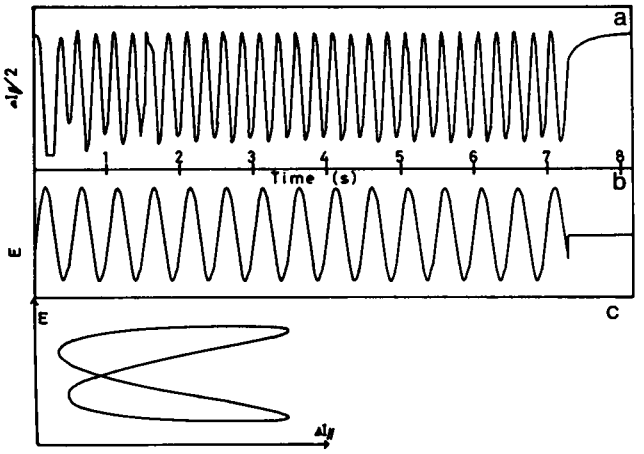

FIGURE 5 Electric dichroism in a sinusoidal electric field. (*a*) Typical time course of $\Delta I_\parallel$. (*b*) Applied electric field (E_0 = 5 V/cm). (*C*) A typical Lissajou's figure formed by taking $\Delta I_\parallel$ and the electric field to the horizontal and vertical axes.

the electric field was plotted against the dichroism change (Fig. 5*c*). It showed a typical Lissajou's figure of frequency ratio 2. Mathematically,

$$y = E = E_0\cos\omega t;\ x = -\Delta I_\parallel = -b\cos(2\omega t - \delta). \quad (23)$$

Therefore, the crossing point ($y = 0$) is described as $x = b\cos\delta$. The normalized b and δ obtained by analyzing data were plotted in Fig. 6. The theoretical curves for normalized b and δ were also calculated according to Eqs. 18 and 19 by substituting the relaxation time after the square electric field was switched off to τ in these equations. The theoretical predictions seem to be good. Furthermore, we repeated this experiment for different sizes of purple membranes and all dispersions were precisely predicted by their relaxation times. Therefore, we concluded that the electric field did not affect the angle factor Θ under our conditions. The conclusion that the orientation of the chromophore within the purple membrane was not affected is consistent with the result that the chromophore is highly immobilized in the membrane, as shown by Razi

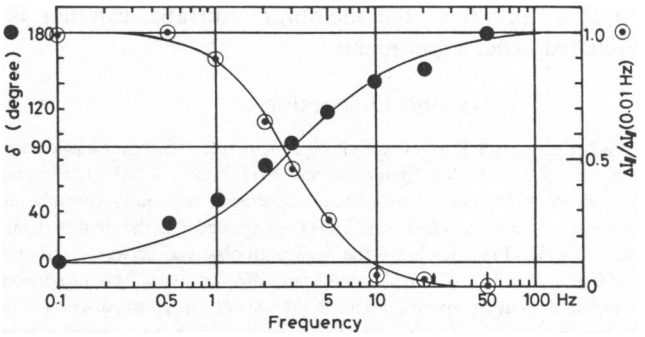

FIGURE 6 Phase delay and amplitude of the electric anisotropy plotted against the frequency. The phase delay was determined from the Lissajou's figure in Fig. 5. Theoretical predictions by using the relaxation time after a square electric field was switched off are also shown (decay time was 21 ms for this sample).

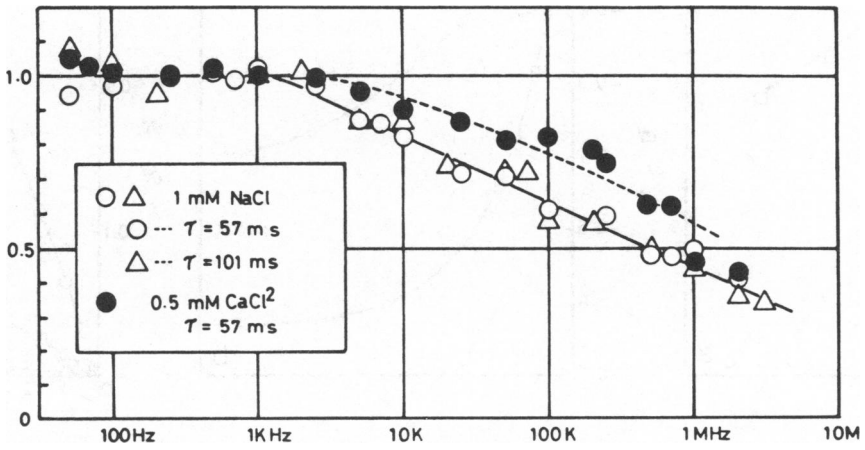

FIGURE 7 The second dispersion of the electric dichroism of purple membrane suspension. The dispersions measured under different conditions were normalized at values between 50 Hz and 1 KHz.

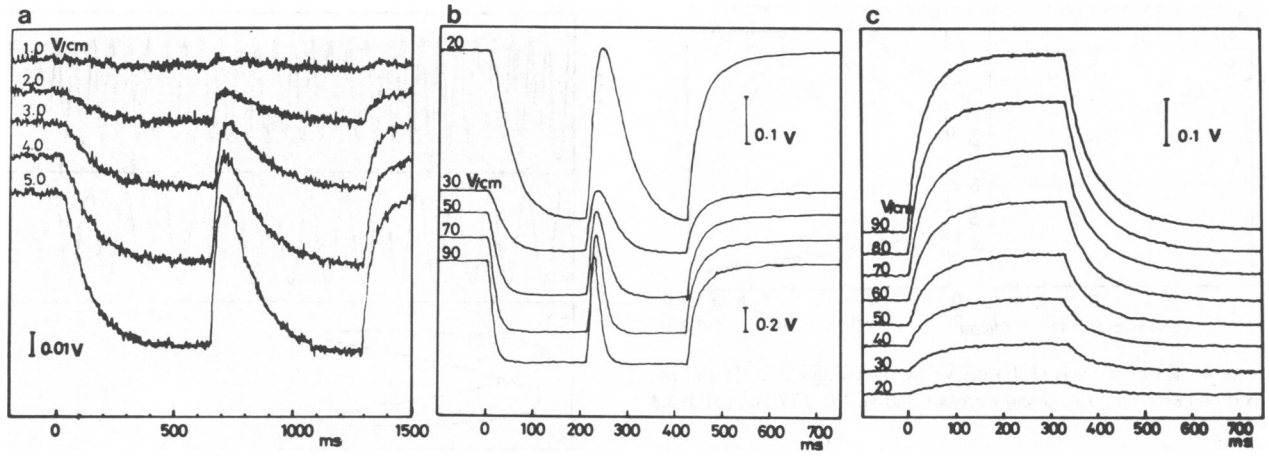

FIGURE 8 Voltage dependence of the time-courses of the electric dichroism of purple membrane suspensions. These were measured at 0.77 Hz (*a*) and (*b*), and at 393.4 Hz (*c*).

Naqvi et al. (19) and by Kouyama et al. (20). But note that the electric dichroism is related only to the angle γ. The possibility, therefore, that the chromophore moves around an axis normal to the membrane surface, can not be excluded in our experiments.

The Second Dispersion

Another dispersion in electric dichroism of purple membrane suspension was observed in higher frequency region (2 kHz – 3 MHz). Electric anisotropy of the purple membrane suspension was quite constant at frequencies between 100 Hz and 2 kHz but showed a moderate dispersion above 2 kHz (Fig. 7). Unlike the dispersion observed between ~10 and ~100 Hz, the sizes of purple membrane did not affect this dispersion appreciably, but the species of ions in the solvent shifted the dispersion to higher frequencies. These experiments suggest that the induced dipole moment, which caused the electric dichroism above ~100 Hz, is due to the movement of ions around the membranes.

Determination of Permanent Dipole Moment and Polarizability

The electric anisotropy at equilibrium (i.e., at plateau of each time course of the dichroism in Fig. 8) was proportional to the square of the electric field at both frequencies when the electric field was weak (Fig. 9*a*, *c*). So we could use Eq. 20. The results ranged from 500 *k*D to 10 MD for the permanent dipole moments and from 1×10^{-13} to 1×10^{-11} cm^3 for the polarizabilities.

In measurement, we selected 0.77 and 393 Hz in consideration of the first and the second dispersions. In

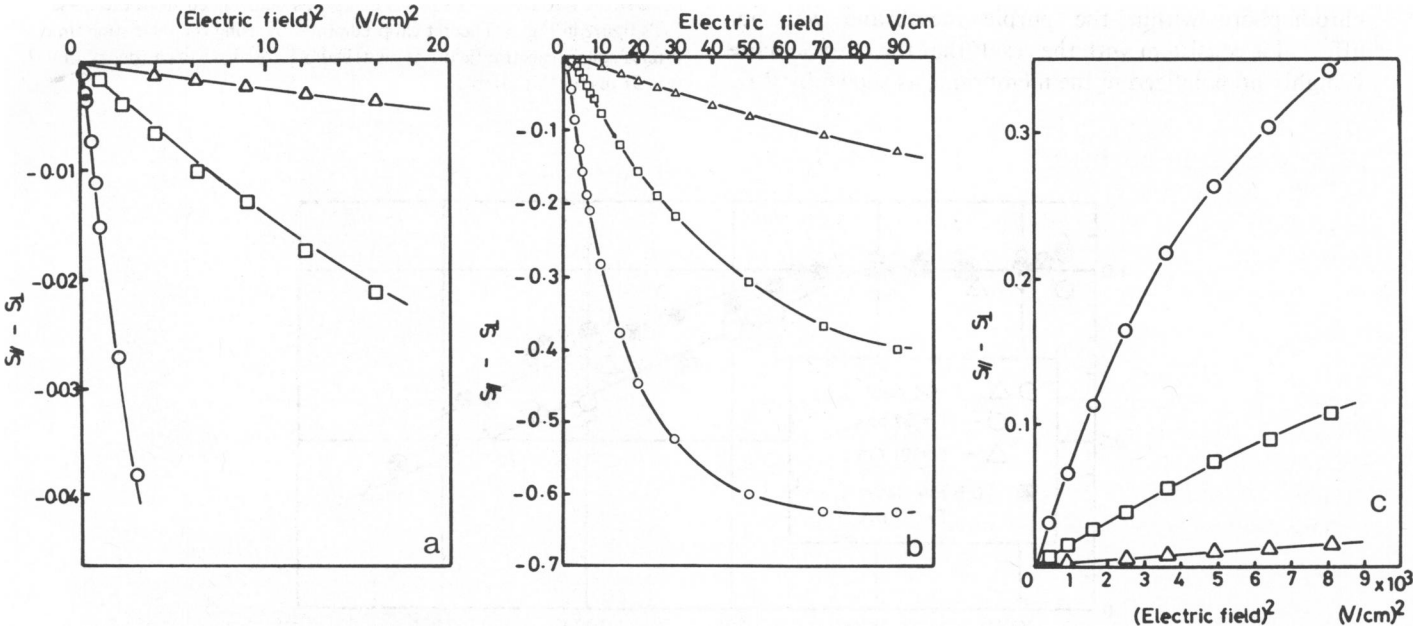

FIGURE 9 Electric anisotropy at equilibrium plotted against the square of the electric field (*a*) and (*c*), and against the electric field (*b*). (*a*, *b*) 0.77 Hz. (*c*) 393.4 Hz. Symbols denote different membrane sizes (see the legend to Fig. 11).

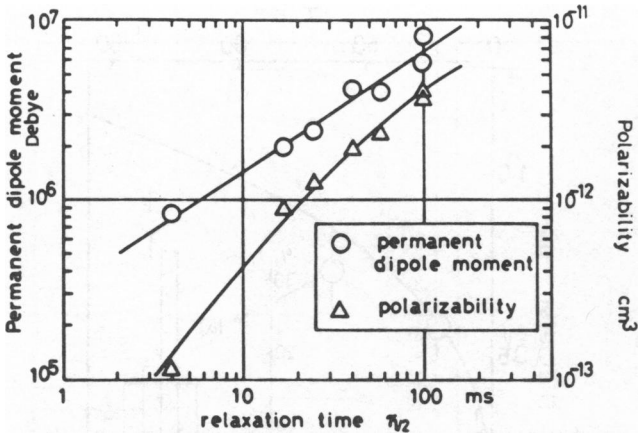

FIGURE 10 Permanent dipole moment and polarizability of purple membranes plotted against the relaxation time.

calculation, we assumed the angle (γ) of retinal against the axis normal to the membrane surface to be 70°, which value is consistent with the angles reported by several authors (21–23). We also could justify this value from the best orientation of purple membranes as follows. The observed highest negative electric anisotropy, $S_{\parallel} - S_{\perp}$, was -0.733 at the low frequency and the highest positive value of the electric anisotropy was 0.45 at the high frequency. So, we obtained

$$0.45 \geq 3 \cdot P_2(\cos\gamma) \cdot \psi \geq -0.733. \qquad (24)$$

Because the orientation factor can take values between -0.5 and 1.0, the above inequality gives $\gamma \geq 68.6°$ and 65.6°. Thus we could show that the angle of retinal against the axis normal to the membrane surface was >68.6°.

Membrane Size Dependence of Permanent Dipole Moment and Polarizability

In log-log scale, both the permanent dipole moment and the polarizability changed according to the relaxation time (Fig. 10). That is, the permanent dipole moment was proportional to the two-thirds power of the relaxation time and the polarizability was almost proportional to the relaxation time. From Perrin's equation (Eqs. 2 and 3), it follows that

$$\mu \propto c^2,$$
$$\alpha_2 - \alpha_1 \propto c^{3\sim4}. \qquad (25)$$

Because the permanent dipole moment was proportional to the square of radius, that is, to the area of the membrane, we could calculate the permanent dipole moment per bacteriorhodopsin: 98 D (SE 10.2 D for seven different lots of purple membranes, 2 – 4 for a single lot [$n = 3 - 8$]).

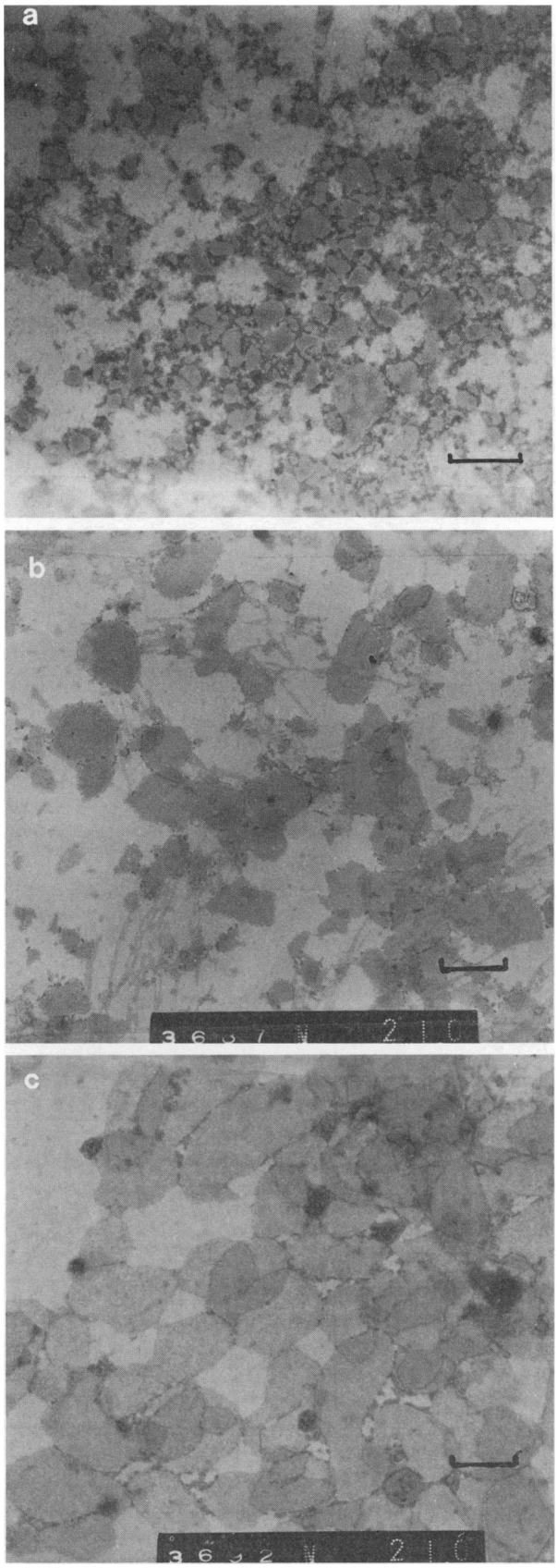

FIGURE 11 Electromicrographs of different membrane sizes. Negative staining. Scale bar in each picture is 0.5 μm. Each relaxation time and the symbol in Fig. 9 are as follows: (*a*) τ = 6.05 ms, Δ in Fig. 8, (*b*) τ = 91.36 ms, □ in Fig. 8, (*c*) τ = 135 ms, ○ in Fig 8.

Confirmation of Perrin's Equation between the Relaxation Time and the Membrane Size

Membrane sizes could be well predicted from relaxation times by Perrin's equation (Eqs. 2 and 3) (Fig. 12). Deviation at the large diameter may come from the irregular shape of the giant membrane (Fig. 11*c*). Here we should note two points for these measurements. First, although our samples were relatively homogeneous, they were not perfect. However, the residual heterogenity was counted in the weight function when we calculated the average diameter (see Materials and Methods). Second, the concentration of purple membranes affected the relaxation time. At high concentration ($\geq$1.0 absorption at 570 nm), the relaxation time increased. The reason may be interaction between the membrane sheets. To decrease this effect, we measured the electric dichrosim at a concentration of absorption 0.3 (<0.4).

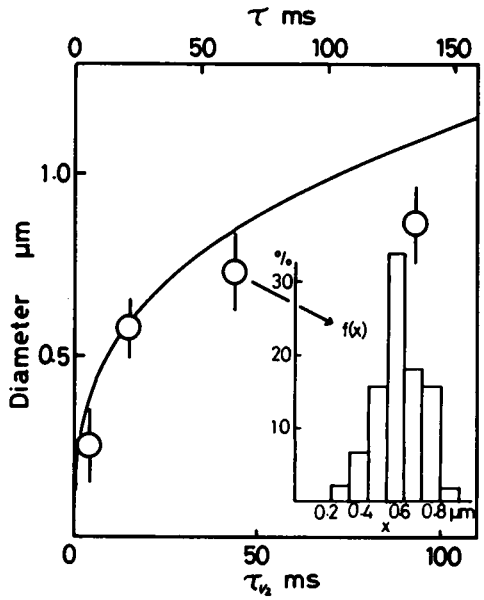

FIGURE 12 Relation between average diameters of purple membranes determined from electronmicrographs and their relaxation time. $f(x)$ is an example of the distribution function. Diameters are weighted average (see Materials and Methods). *Curve* shows Perrin's theoretical curve.

Salt Effects on Permanent Dipole Moment and Polarizability

Both the permanent dipole moment and the polarizability decreased as the ionic strength increased (Fig. 13). In the case of the permanent dipole moment, ionic species, Ca^{2+} and Na^{+}, had different effects. Ca^{2+} had a large effect at low concentrations, where Na^{+} had only moderate effect. In the case of the polarizability, ionic species did not have different effects. All relaxation curves in these experiments could be superimposed, so the possibility of morphological changes, for instance, aggregation or shrinking, can be excluded.

Effects of Trypsin Treatment on the Permanent Dipole Moment

The permanent dipole moment of bacteriorhodopsin decreased when the purple membranes were treated with trypsin (Fig. 14). As the time of trypsin treatment increased, the permanent dipole moment tended to saturate around 74/bacteriorhadopsin. Because the trypsin treatment removed one negative charge from the cytoplas-

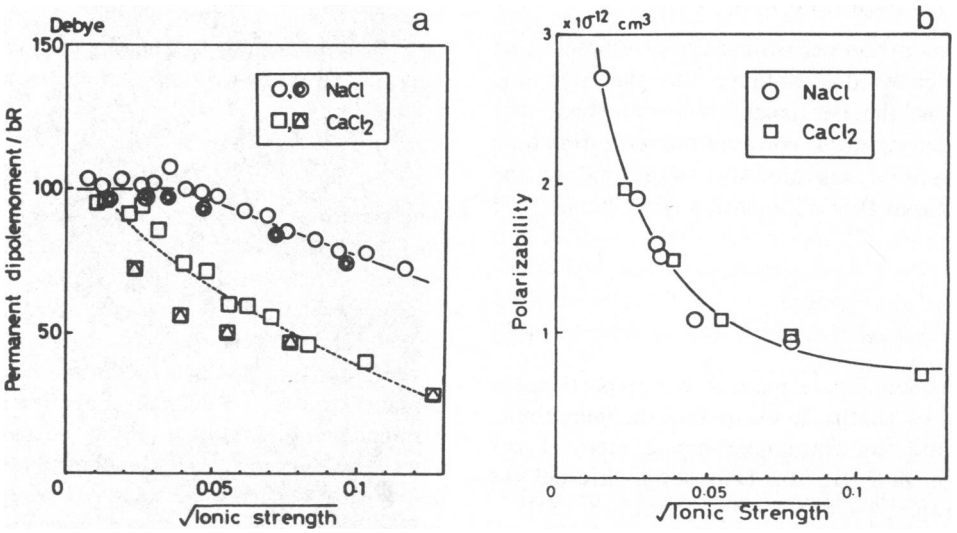

FIGURE 13 Dependence of permanent dipole moment and polarizability on ionic strength. These were measured in the presence of 0.1 mM phosphate buffer (pH 7.0), which was also counted into the ionic strength. (*a*) Permanent dipole moment. Simple symbol: τ = 89.5 ms. Double symbol: τ = 57.7 ms. bR, bacteriorhodopsin. (*b*) Polarizability. τ = 57.7 ms.

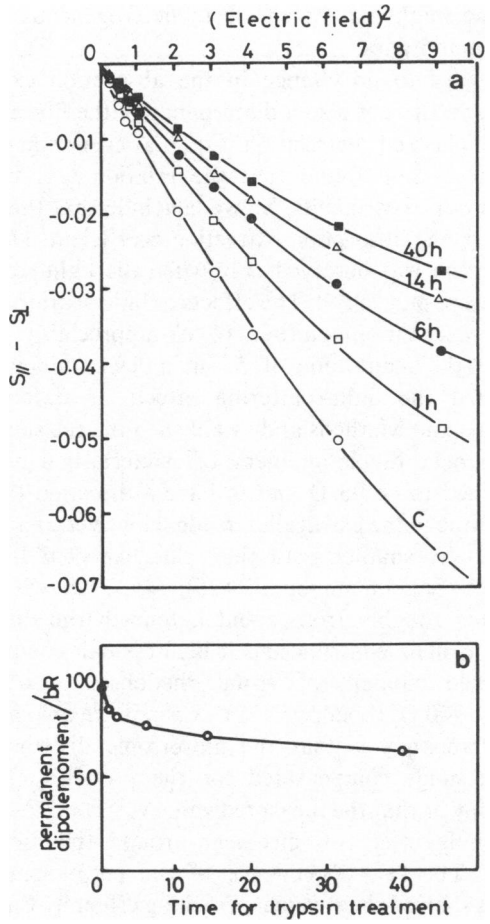

FIGURE 14 Effect of trypsin digestion on the permanent dipole moment of bacteriorhodopsin (bR).

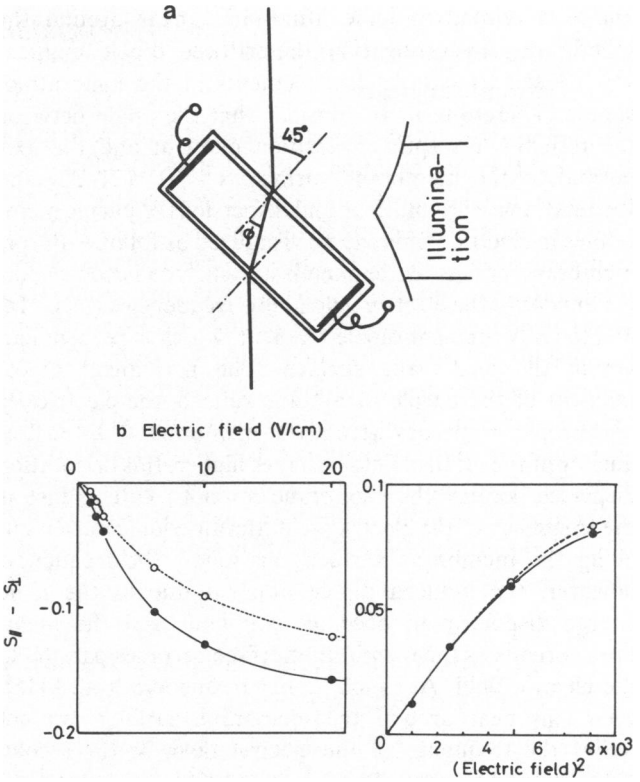

FIGURE 15 (*a*) Optical configuration for measuring the electric dichroism under illumination. (*B*) Effects of illumination on the electric anisotropy. (O) Under illumination; (●) in the dark.

mic side of bacteriorhodopsin (24), we concluded that the direction of the permanent dipole momemt was from the cytoplasmic to the outer side. However, the final state was equivocal possibly due to another weak cleavage-site. Therefore, we determined the number of removed amino acid terminals by using the fluorescent probe, fluorescamine, and found that the ratio of the amino terminal to bacteriorhodopsin was a little larger than one after 40 h of the treatment. But the difference was relatively small and the reproducibility ($n = 4$) was good, so we concluded that the major cleavage site was the same as those of reported ones. In these experiments, again, the relaxation times were the same as those of control samples.

Change of the Permanent Dipole Moment During the Photoreaction Cycle

Under illumination, the electric anisotropies decreased at the low frequency (0.77 Hz) and did not change at the high frequency (393 Hz) (Fig. 15*b*). At the same time, the absorption at 570 nm decreased to 71.8% of the original absorption. We calculated the number of bacteriorhodopsin under the photoreaction cycle from this absorption change. In the calculation, we used the average extinction coefficient at 570 nm of bacteriorhodopsin under the photoreaction cycle, 15,200, which was calculated according to reference 25. Thus, we calculated the number of bacteriorhodopsin under the photoreaction cycle and could determine the change of the dipole moment per bacteriorhodopsin, from 98 to 63.3 Debye/bacteriorhodopsin (SE 3.7 D).

DISCUSSION

The electric anisotropy of a purple membrane suspension shows negative or positive values depending on the frequency of the electric field applied to the suspension; negative below ~10 Hz and positive above ~100 Hz. The change of electric anisotropy at lower frequencies (≤10 Hz) had characteristics of permanent dipole moment orientation and the change at higher frequencies (≥100 Hz) had characteristics of induced dipole moment orientation. The dispersion of the permanent dipole moment orientation occurred between 10 and 100 Hz and was predicted precisely by the rotational relaxation of the membrane sheets. No change in angle factor was also shown in this analysis. The dispersion of the induced dipole moment orientation occurred above 2 kHz up to 3 MHz

and was related to ionic atmosphere near around the membrane, suggesting that the induced dipole moment was caused by charge displacements in the ionic atmosphere. Therefore, if we consider that the angle between the retinal's absorption transition moment and the axis normal to the membrane surface is ~70° (21–23, and Results), these orientations and dispersions of purple membranes in electric fields can be visualized as follows. Purple membrane orients as the membrane surface becomes perpendicular to the electric field at low frequencies (≤10 Hz) due to its permanent dipole moment, which is perpendicular to the membrane surface. The permanent dipole moment of the purple membrane reflects the electrically anisotropic properties across the membrane. As the frequency of the electric field becomes higher, this orientation dispersed because the membrane can not rotate as fast as the frequency of the electric field. Because ionic movement along the membrane surface can follow the frequency, however, the induced dipole moment due to the ionic charge displacement becomes dominant and the membrane orients as the membrane surface becomes parallel to the electric field. At much higher frequencies (≥2 kHz), even ions near around the membrane surface can not follow the frequency of the electric field, so the second orientation disperses. This interpretation was suggested previously (11) and is now confirmed.

As for no change in the angle factor within the purple membrane, there is a discrepancy in the literature. Shinar et al. (6) and Druckmann and Ottolenghi (9) applied a high electric field (~10 kV/cm) to a suspension of purple membranes, and all of them observed both a fast relaxation time (~300 μs) and a slow relaxation time (~100 ms [6, 9]; 3 ms [10]). They attributed the fast relaxation time to the chromophore rotation. However, Saigo (7), Keszthelyi (8), and Kimura et al. (11) observed only the slow relaxation time. By analyzing the dispersion mechanism, we also conclude that the angle factor does not change. Three possible explanations for this discrepancy are as follows. First, the chromophore rotation may have been induced by the high electric field. However, the voltage (~10 kV/cm) corresponds to ~5 mV/50A. This value is not so high in comparison to the membrane potential difference under biological conditions. A possible explanation may be that a heterogeneous electric field around the purple membrane made the local electric field intensity strong enough to induce the chromophore rotation. Second, the fast relaxation time might come from a residual electric field after the electric field is switched off. The actual electric field in a suspension can be distorted considerably due to the electrode polarization. This electrode's polarization sometimes leaves a residual electric field after the electric field is switched off. This possibility should be checked under the conditions used in the high voltage experiments. When we used fresh platinized platinum electrodes, the residual electric field was reasonably small. Third, the fast relaxation time might have come from heterogeneous sizes of purple membranes.

In regard to no change in the absorption extinction coefficient, there is also a discrepancy in the literature (8, 10). We checked the relation, Eq. 5, at every stage of our experiments and found that the relation was valid all through our experiments. So we conclude that there is no change in the absorption extinction coefficient. However, this relation was observed only when the light-scattering effects were minimized. The effects of light scattering were to decrease the magnitude of $S_{\parallel}$ appreciably and to increase the magnitude of $S_{\perp}$ in a lesser amount. We minimized the light-scattering effects as described in Materials and Methods and established the relation.

Permanent dipole moment of bacteriorhodopsin was determined to be 98 D and to have a direction from the cytoplasmic to the extracellular side. However, this value is substantially smaller than the value expected from the model of Engelmann et al. (26), ~500 D, which was calculated roughly from about a four-charge difference and the α-helix contribution. It is also small compared to the dipole moment of visual rhodopsin in detergent micelles, 720 D/rhodopsin (27). A possible explanation for this discrepancy is that the anisotropic distribution of charged lipids compensated for the protein's electrical anisotropy or that the measured value was compensated by a screening effect of ions near around the membrane surface. The salt dependence of the permanent dipole moment showed the stronger screening effect by Ca^{2+} than that by Na^{+}.

We estimated such a screening effect by the trypsin treatment and showed that one charge difference corresponded to 24 D/bacteriorhodopsin, suggesting a four-charge difference from 98 D/bacteriorhodopsin. Although this estimation has some ambiguities, still it may give the first approximation of the screening effect. Major ambiguities are as follows. First, the charge cutoff by the trypsin treatment may not be a good representative of charges on the side because the specific charge has a specific location and a specific ion distribution near the location. Second, the ratio of dipole moment to charge may not be valid for the entire number of charges; in other words, the removal of the second charge from the same side might have a different ratio of dipole moment to charge. Third, removal of the C-terminal residues may change the conformation of the protein. Finally, the trypsin treatment itself seems to have some unspecificity.

During the photoreaction cycle, the permanent dipole moment decreased by 34.7 D/bacteriorhodopsin. Because the charge movement near the membrane surface was shown to be faster than 2 kHz (Fig. 7), which is fast enough in comparison to the lifetimes of the photoreaction intermediates, *M* (1 ms), *N* (4 ms), and O (5 ms), we may assume the same screening effect estimated by the trypsin treatment. Therefore, the change of permanent dipole

moment suggests that a dynamic change of charge distribution across the membrane occurred during the photoreaction cycle.

In this article we report the permanent dipole moment and the polarizability of purple membranes in suspension. We have been able to show that (*a*) the mechanism of two dispersions, (*b*) the existence of local ions, (*c*) the local ions move faster than 2 kHz (the second dispersion), (*d*) the screening effect due to the local ions is quite large (trypsin treatment experiment), and (*e*) the dynamic change of the permanent dipole moment occurs during the photoreaction cycle.

We want to thank Drs. K. Kinosita, Jr., K. Ohno, S. Saigo, and Y. Takeuchi for their helpful discussions. We also thank Drs. E. Yamada and J. Usukura for taking electronmicrographs of our samples, Dr. Ando, Dr. Ikawa and the late Dr. Hayase for letting us use instruments to purify samples, and Mrs. K. Nakajima for her helpful assistance. We appreciate Ms. M. Zeiger's helpful discussion during the preparation of this article. We also thank Dr. W. Stoeckenius for his generous help in revising the manuscript.

This work was supported by a Research Grant for Solar Energy Conversion–Photosynthesis from the Science and Technology Agency of Japan, and by grants in aids for scientific research from the Ministry of Science, Culture and Education of Japan.

This paper is a part of the Ph.D. thesis submitted to the University of Tokyo in February, 1981, by Dr. Kimura.

Received for publication 31 August 1982 and in final form 21 September 1983

REFERENCES

1. Oesterhelt, D., and W. Stoeckenius. 1971. Rhodopsin-like protein from the purple membrane of *Halobacterium halobium*. *Nat. New Biol.* 233:149–152.
2. Oesterhelt, D., and W. Stoeckenius. 1973. Functions of a new photoreceptor membrane. *Proc. Natl. Acad. Sci. USA* 70:2853–2857.
3. Henderson, R. 1977. The purple membrane from Halobacterium halobium. *Annu. Rev. Biophys. Bioeng.* 6:87–109.
4. Stoeckenius, W., R. H. Lozier, and R. Bogomolni. 1979. Bacteriorhodopsin and the purple membrane of halobacteria. *Biochim. Biophys. Acta.* 505:215–278.
5. Stoeckenius, W., and R. Bogomolni. 1982. Bacteriorhodopsin and related pigments of halobacteria. *Annu. Rev. Biochem.* 52:587–615.
6. Shinar, R., S. Druckmann, M. Ottolenghi, and R. Korenstein. 1977. Electric fields effect in bacteriorhodopsin. *Biophys. J.* 19:1–5.
7. Saigo, S. 1978. The orientation of purple membranes in electric field. *In* Biological and Chemical Utilization of Solar Energy. Gakkai Shuppan Center, Tokyo. 127–131.
8. Keszthelyi, L., 1980. Orientation of membrane fragments by electric field. *Biochim. Biophys. Acta.* 598:429–436.
9. Druckmann, S., and M. Ottolenghi. 1981. Electric dichroism in the purple membrane of *Halobacterium halobium*. *Biophys. J.* 33:263–268.
10. Tsuji, K., and E. Neumann. 1981. Structural change in bacteriorhodopsin induced by electric impulses. *Int. J. Biol. Macromol.* 3:231–242.
11. Kimura, Y., A. Ikegami, K. Ohno, S. Saigo, and Y. Takeuchi. 1981. Electric dichroism of purple membrane suspensions. *Photochem. Photobiol.* 33:435–439.
12. Oesterhelt, D., and W. Stoeckenius, 1974. Isolation of the cell membrane of *Halobacterium halobium* and its fractionation into red and purple membranes. *Methods Enzymol.* 31:667–678.
13. Gerber, G. E., C. P. Gray, D. Wildenauer, and H. G. Khorana. 1977. Orientation of bacteriorhodopsin in *Halobacterium halobium* as studied by proteolysis. *Proc. Natl. Acad. Sci. USA.* 74:5426–5430.
14. Perrin, F. 1934. Mouvement brownien d'un ellipsoïde I Dispersion diélectrique pour des molecules ellipsoïdales. *J. Phys. Radium.* 5:497–511.
15. Unwin, P. N. T., and R. Henderson. 1975. Molecular structure determination by electronmicroscopy of unstained crystalline specimens. *J. Mol. Biol.* 94:425–440.
16. Benoit, H. 1951. Contribution a l'étude de l'effet Kerr presenté par les solutions Dilus de macromolécules rigides. *Ann. Phys.* 6R:561–609.
17. Ogawa, S., and S. Oka. 1960. Theory of electric birefringence in dilute solutions of tobacco mosaic virus. *J. Physiol. Soc. Jpn.* 15:658–668.
18. Shah, M. J. 1963. Electric birefringence of Bentonite II. An extension of saturation birefringence theory. *J. Phys. Chem.* 67:2215–2219.
19. Razi Naqvi, K., Gonzales-Rodriquez, J., Cherry, R. J. and Chapman, D., 1973. Spectroscopic technique for studying protein rotation in membranes. *Nat. New Biol. 245:249–251.*
20. Kouyama, T., Y. Kimura, K. Kinosita, Jr., and A. Ikegami. 1981. Immobility of the chromophore in bacteriorhodopsin. *FEBS* (*Fed. Eur. Biochem. Soc.*) *Lett.* 124:100–104.
21. Heyn, M. P., R. J. Cherry, and U. Muller. 1977. Transient and linear dichroism studies on bacteriorhodopsin: determination of the orientation of the 568 nm all *trans* retinal chromophore. *J. Mol. Biol.* 117:607–620.
22. Bogomolni, R. A., S. B. Hwang, Y. W. Tseng, G. I. King, and W. Stockenius. 1977. Orientation of the bacteriorhodopsin transition dipole. *Biophys. J.* 17:98a. (Abstr.)
23. Korenstein, R., and B. Hess. 1978. Immobilization of bacteriorhodopsin and orientation of its transition moment in purple membrane. *FEBS* (*Fed. Eur. Biochem. Soc.*) *Lett.* 89:15–20.
24. Ovchinnikov, Yu. A., N. G. Abdulaev, M. Y. Feigna, A. V. Kiselev, and N. A. Lobanov. 1979. The structural basis of the functioning of bacteriorhodopsin: an overview. *FEBS* (*Fed. Eur. Biochem. Soc.*) *Lett. 100:219–244.*
25. Lozier, R. H., R. A. Bogomolni, and W. Stoeckenius. 1975. Bacteriorhodopsin: a light driven proton pump in *Halobacterium halobium. Biophys. J.* 15:955–962.
26. Engelmann, D. M., R. Henderson, A. D. McLachlen, and B. A. Wallace. 1980. Path of the polypeptide in bacteriorhodopsin. *Proc. Natl. Acad. Sci. USA* 77:2023–2027.
27. Petersen, D. C., and R. A. Cone. 1975. The electric dipole moment of rhodopsin solubilized in triton X-100. *Biophys. J.* 15:1181–1200.